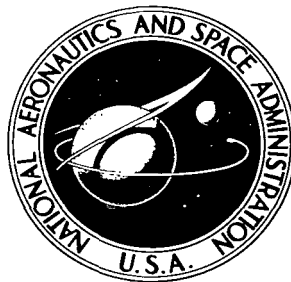


NASA TECHNICAL NOTE



NASA TN D-2706

e. 1

LOAN COPY: 1  
AFWL (V  
KIRTLAND A

0079753



TECH LIBRARY KAFB, NM

NASA TN D-2706

EFFECTS OF SURFACE EMITTANCE  
ON TURBULENT SKIN FRICTION AT  
SUPERSONIC AND LOW HYPERSONIC SPEEDS

*by Jerry M. Allen and K. R. Czarnecki*

*Langley Research Center*

*Langley Station, Hampton, Va.*



0079753

EFFECTS OF SURFACE EMITTANCE ON TURBULENT SKIN FRICTION  
AT SUPERSONIC AND LOW HYPERSONIC SPEEDS

By Jerry M. Allen and K. R. Czarnecki

Langley Research Center  
Langley Station, Hampton, Va.

NATIONAL AERONAUTICS AND SPACE ADMINISTRATION

---

For sale by the Office of Technical Services, Department of Commerce,  
Washington, D.C. 20230 -- Price \$2.00

# EFFECTS OF SURFACE EMITTANCE ON TURBULENT SKIN FRICTION

## AT SUPERSONIC AND LOW HYPERSONIC SPEEDS

By Jerry M. Allen and K. R. Czarnecki  
Langley Research Center

### SUMMARY

A search of available literature indicates that the radiative properties of supersonic aircraft materials depend heavily upon the metal chosen for the aircraft skin and the degree of oxidation of the surface. A calculative study has been made to determine the effect of emittance upon wall temperature and skin friction over a range of supersonic and low hypersonic flight conditions. Calculations were made for Mach numbers up to 9, altitudes up to 80 000 feet, and vehicle lengths up to 200 feet.

The results indicate that the skin-friction drag of a supersonic aircraft increases with increased surface emittance. Emittance increases with surface oxidation. Thus, for a new supersonic aircraft with skin made of a metal with low radiative properties in the polished, unoxidized state, the skin-friction drag will increase with time until the surface becomes stably oxidized. This effect of emittance on skin friction increases with Mach number and becomes substantial above Mach numbers of about 2.5. Hence, for specified flight conditions, the level of skin-friction drag at which the vehicle operates depends upon the metal used for the skin of the aircraft and the degree of oxidation of the metal.

### INTRODUCTION

A body flying at supersonic speeds develops a skin-friction drag which, for given flight conditions, is a function of the wall temperature. The wall temperature, in turn, is dependent upon the ability of the aircraft surface to radiate part of the energy which it receives through aerodynamic heating back to the atmosphere. This ability to radiate energy is described by a quantity known as emittance, which is defined as the ratio of the rate of radiant emission from a body, as a consequence of its temperature only, to the corresponding rate of emission from a blackbody at the same temperature. The range of  $\epsilon$  is between 0 and 1, where  $\epsilon = 0$  represents a nonradiating body and  $\epsilon = 1$  represents a perfect radiator (blackbody).

In performing skin-friction calculations for full-scale flight conditions, the usual procedure is to choose a value of emittance (usually about 0.85) and to assume that this value holds for all metals and remains constant throughout

the life of the aircraft. A search of available literature, however, revealed that surface emittance for supersonic aircraft materials can vary widely with the degree of surface oxidation and with the metal used for the skin of the aircraft. (See fig. 1.) Therefore, the present investigation was undertaken to determine the effect of emittance upon wall temperature and skin friction over a range of supersonic and low hypersonic flight conditions. Although it is evident that the effects of emittance on skin temperature and structural considerations heavily outweigh any effects on skin-friction drag, the object of this paper is to point out that these effects on drag do exist and to provide for a quantitative assessment of them. Calculations were made for Mach numbers up to 9, altitudes up to 80 000 feet, and vehicle lengths up to 200 feet.

All calculations are for two-dimensional, fully turbulent flow over a flat plate. Air is assumed to be a perfect gas and a continuous medium. The errors associated with this assumption are negligible at the lower Mach numbers but become more pronounced at the higher Mach numbers ( $M > 7$ ).

As an aid to aircraft designers in making wall-temperature calculations a number of design charts have been derived and are presented in an appendix. These design charts contain detailed plots of the effects of emittance, Mach number, and altitude on the distribution of equilibrium wall temperatures for vehicle lengths up to 200 feet.

#### SYMBOLS

$C_F$	local skin-friction coefficient
$c_p$	specific heat of air at constant pressure (0.24 Btu/lb-°R)
$C_F$	average skin-friction coefficient
$h$	coefficient of heat transfer, Btu/ft <sup>2</sup> -°R-sec
$H$	altitude, ft
$L$	body length, ft
$M$	Mach number
$V$	velocity, ft/sec
$R/\text{ft}$	Reynolds number per foot, $\frac{\rho_\infty V_\infty}{\mu_\infty}$
$q$	heat-transfer rate per unit area, Btu/sec-ft <sup>2</sup>
$T$	temperature, °R

x	longitudinal distance, ft
$\epsilon$	emittance
$\gamma$	ratio of specific heats (1.4 for air)
$\eta$	temperature recovery factor (0.88 for turbulent boundary layer)
$\rho$	density of air, lbm/ft <sup>3</sup>
$\sigma$	Stefan-Boltzmann constant ( $0.483 \times 10^{-12}$ Btu/sec-ft <sup>2</sup> -°R <sup>4</sup> )
$\mu$	coefficient of viscosity $\left(0.232435 \times 10^{-7} \frac{T_{\infty}^{1.5}}{T_{\infty} + 216}\right), \frac{\text{lbf-sec}}{\text{ft}^2}$

#### Subscripts:

a	aerodynamic
r	radiative
w	wall conditions
$\infty$	free-stream conditions
aw	adiabatic wall conditions
L/2	conditions at the midpoint of the body

#### METHOD OF CALCULATION

The wall temperatures presented in this paper were calculated by forming a heat balance between aerodynamic and radiative heating as described in reference 1. The aerodynamic heat input to a surface of unit area is given by

$$q_a = h(T_{aw} - T_w) \quad (1)$$

The radiative heat lost by the surface is given by

$$q_r = \epsilon \sigma T_w^4 \quad (2)$$

For no net heat-transfer rate the aerodynamic and radiative terms must be equal. Hence,

$$q_a = q_r \quad (3)$$

$$h(T_{aw} - T_w) = \epsilon \sigma T_w^4 \quad (4)$$

$$\frac{\epsilon \sigma}{h} T_w^4 + T_w = T_{aw} \quad (5)$$

but

$$T_{aw} = T_\infty \left( 1 + \frac{\gamma - 1}{2} \eta M_\infty^2 \right) \quad (6)$$

and

$$h = 0.6 C_f c_p \rho_\infty V_\infty \quad (7)$$

Finally,

$$\frac{\left( 0.1043 \times 10^{-12} \frac{\text{lb-sec}}{\text{ft}^3 \cdot \text{R}^3} \right) \epsilon T_w^4}{\mu_\infty C_f R / \text{ft}} + T_w = T_\infty \left( 1 + 0.176 M_\infty^2 \right) \quad (8)$$

Equation (8) shows that the equilibrium wall temperature is a function of Mach number, Reynolds number, altitude, and surface emittance. All skin-friction coefficients used in this report were estimated by the modified T' method described in reference 2. The range of values of  $\epsilon$  used in the calculations was based on the results of references 3 to 8. Equation (8), because it requires a double iterative process, is very tedious to solve by hand; hence, an electronic data processing machine (IBM 7094) was utilized to make the wall-temperature and skin-friction calculations.

The calculations neglect the solar radiation heat impinging upon the upper surface of the aircraft during daytime operation. Sample calculations for a heat balance between aerodynamic, radiative, and solar terms indicate that the errors associated with neglecting the solar term are negligible even under the most severe solar conditions - noontime flying of a highly absorptive vehicle at high altitudes. In addition, it was assumed that no conductive heat transfer occurred between the surface and the interior of the aircraft. Reference 9 has reported that this assumption is not unreasonable.

## RESULTS AND DISCUSSION

The variation of emittance with wall temperature for a typical stainless-steel specimen shows that the ability of steel to radiate energy increases considerably with the degree of surface oxidation. (See fig. 1(a), prepared from refs. 3 and 4.) The lower curve ( $\epsilon \approx 0.1$ ) might represent the radiative characteristics of a supersonic aircraft before it had been flown and exposed to aerodynamic heating. The highest curve ( $\epsilon \approx 0.9$ ) would probably represent the

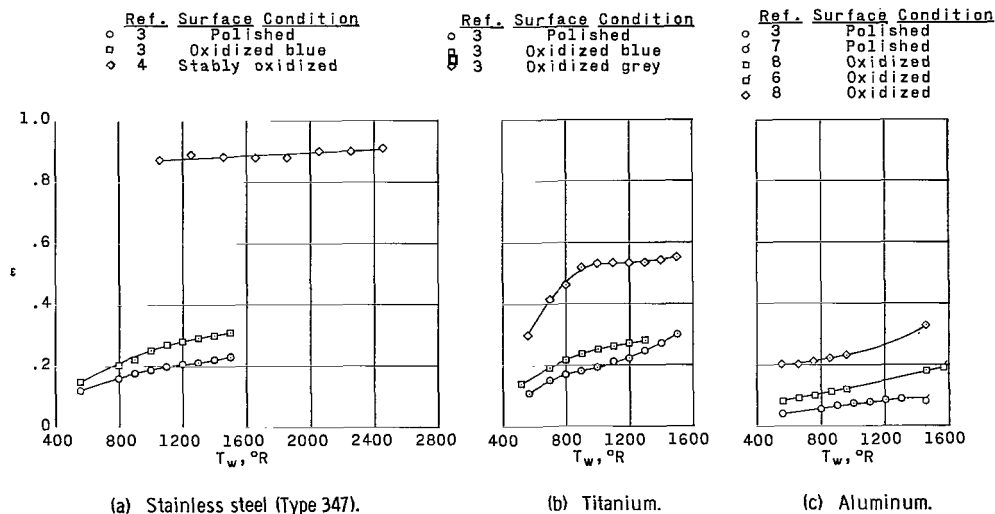


Figure 1. - Effect of wall temperature on surface emittance.

characteristics of a vehicle which had been oxidized by exposure to aerodynamic heating for several supersonic flights.

Figure 1(b) shows the radiative properties of a typical titanium specimen (ref. 3). The same trend of emittance with surface condition is displayed, but the level of emittance reached by the oxidized titanium ( $\epsilon \approx 0.5$ ) is not nearly so high as that reached by the oxidized stainless steel.

The radiative properties of aluminum (fig. 1(c), prepared from refs. 3, 6, 7, and 8) reveal that the emittance of aluminum remains at a relatively low level (below  $\epsilon = 0.3$ ) even after its surface has been oxidized.

Hence, the radiative properties of supersonic-aircraft metals vary widely. In this paper the emphasis is on the radiative properties of stainless steel and titanium. In general, aluminum is not discussed because its physical properties forbid its use as an aircraft surface material above Mach numbers of about 2.2, and at Mach numbers below 2.2 the effects of emittance are small.

Equation (8) shows that, for given flight conditions, the value of emittance of a metal determines the skin temperature of the vehicle. The temperature, in turn, determines the skin-friction drag on the vehicle. To evaluate the magnitude of the effect of surface emittance on skin-friction drag, a computer program was utilized to calculate wall temperature and flat-plate skin friction for a variety of flight conditions and emittance values.

As an aid to aircraft designers in making wall-temperature calculations, a number of design charts have been derived and are presented in an appendix. These design charts contain detailed plots of the effects of emittance, Mach number, and altitude on the distribution of equilibrium wall temperatures for vehicle lengths up to 200 feet.

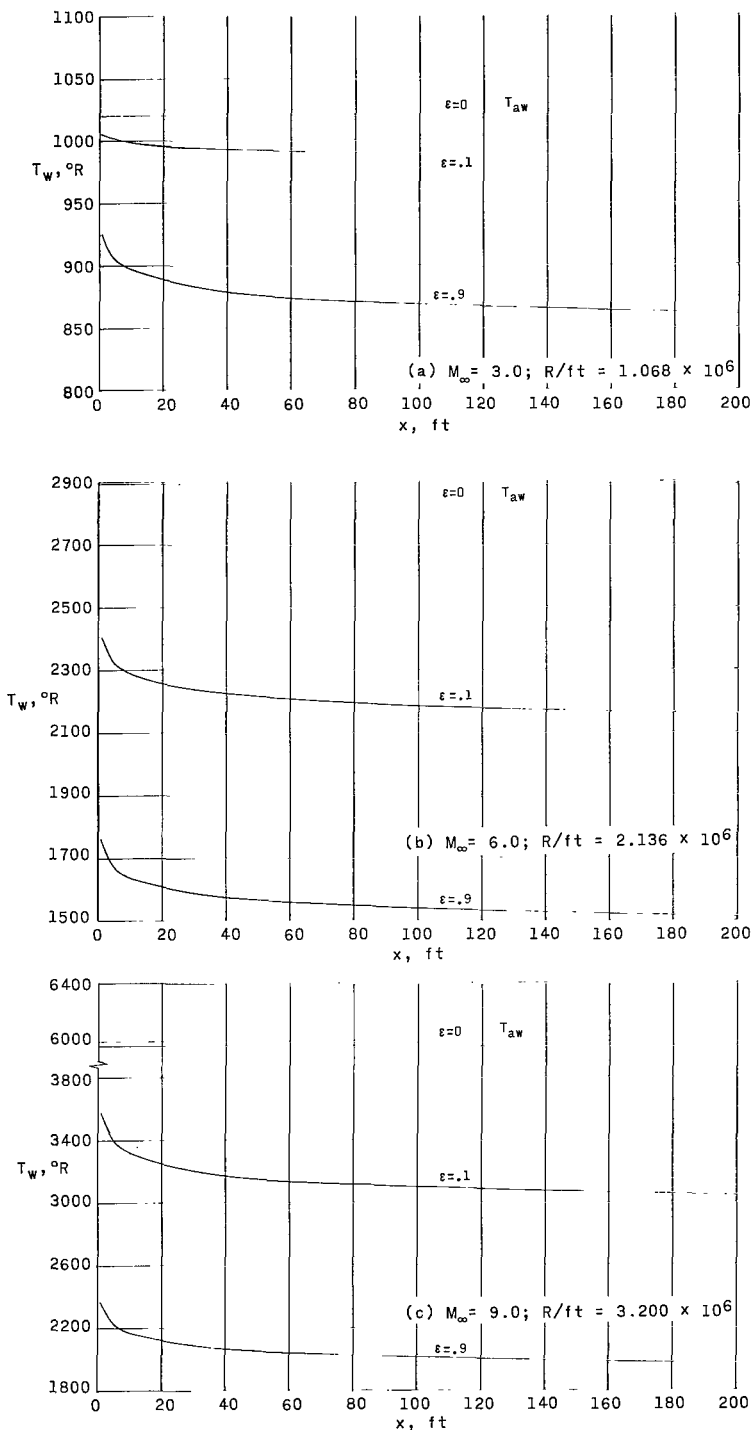


Figure 2 - Variation of wall temperature with longitudinal distance.  
H = 75 000 feet.

Figure 2(a) shows the wall-temperature distribution along a 200-foot-long flat plate flying at 75 000 feet at Mach 3. The horizontal line is the adiabatic-wall-temperature case ( $\epsilon = 0$ ). Increasing emittance causes a decrease in wall temperature. The temperature decrease is desirable from strictly thermal considerations, but, as will be noted subsequently, is detrimental from a skin-friction consideration. A decrease in wall temperature leads to an increase in skin friction. Thus, skin friction increases with increased surface emittance. The emittance values of 0.1 and 0.9 were chosen for calculative purposes because they represent the practical limits for aircraft metals. (See fig. 1.)

The steep temperature gradient near the leading edge of the body is explained, mathematically, by the fact that the values of  $C_f$  in equation (8) are very high due to the low Reynolds numbers near the leading edge. Physically, the wall temperature would be expected to rise as the stagnation point on a body is approached. After the initial gradient the temperature tends to level off with increasing distance because, as the Reynolds numbers become larger, the corresponding decreases in  $C_f$  become smaller.

The temperature distributions for Mach numbers 6 and 9 at the same altitude

( $H = 75\,000$  ft) are shown in figures 2(b) and 2(c), respectively. The adiabatic-wall temperature, of course, increases with Mach number, but even an emittance of 0.1 provides a very large reduction in temperature from the adiabatic case at the higher Mach numbers.

The local skin-friction distributions along the flat plate are presented in figures 3(a) to 3(c) and correspond to the temperature distributions shown in figures 2(a) to 2(c). The increase in  $C_f$  near the leading edge is, again, due to the very low Reynolds numbers in this region. The effect of emittance on  $C_f$  becomes increasingly important with increasing Mach number.

In figure 4 the equilibrium wall temperature at the midpoint of the body is plotted against Mach number for several values of emittance. The length of the body is taken to be 200 feet, which is estimated to be the approximate length of future supersonic transport aircraft. The wall temperature begins to diminish significantly from that of the adiabatic wall above a Mach number of about 2.5. At Mach 9 the wall temperature of oxidized stainless steel ( $\epsilon = 0.9$ ) is about  $1100^\circ$  lower than the temperature of polished stainless steel ( $\epsilon = 0.1$ ) and about  $240^\circ$  lower than the temperature of oxidized titanium ( $\epsilon = 0.5$ ).

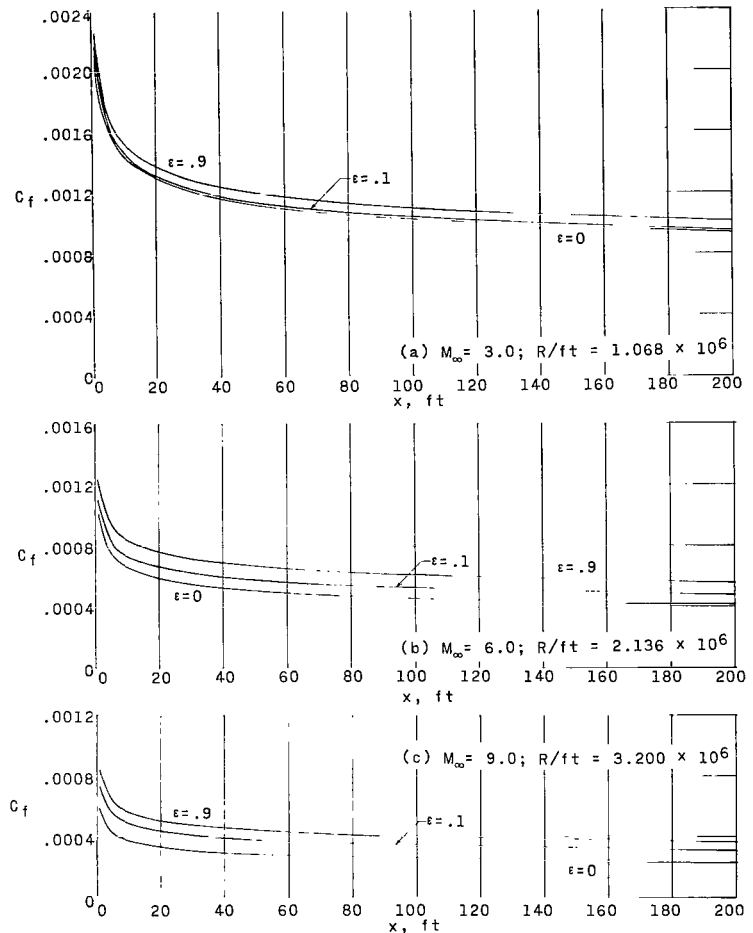


Figure 3. - Variation of local skin-friction coefficient with longitudinal distance.  $H = 75\,000$  feet.

The average skin-friction coefficients, corresponding to the equilibrium wall temperatures of figure 4, are shown in figure 5. For the skin-friction calculations, the wall temperature was assumed to be constant over the entire length of the plate. To show more clearly the effect of emittance on skin friction, figure 6 presents the ratio of  $C_F$  at the given emittance to  $C_F$  at an emittance of zero (adiabatic-wall conditions) plotted against Mach number.

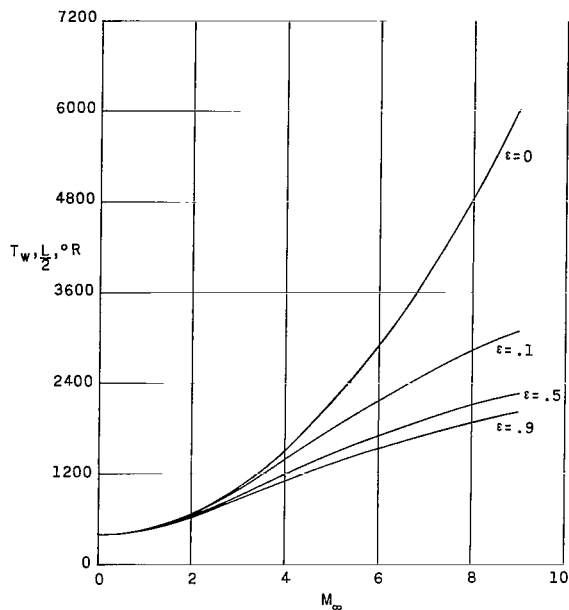


Figure 4. - Variation of equilibrium wall temperature at  $L/2$  with Mach number and emittance.  $H = 75\ 000$  feet;  $L = 200$  feet.

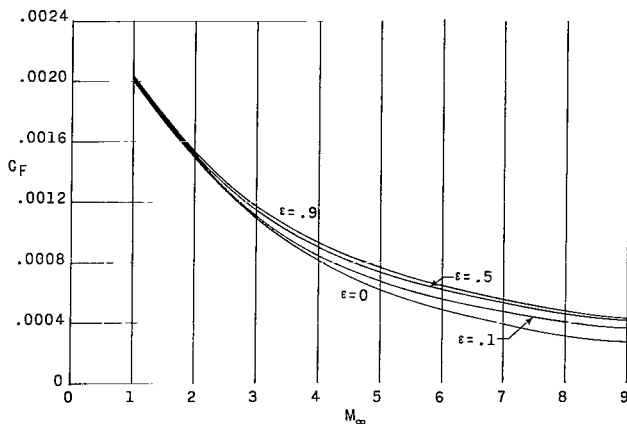


Figure 5. - Effect of emittance and Mach number on average skin-friction coefficient.  $H = 75\ 000$  feet;  $L = 200$  feet.

The change in the slope of the curves at about 40 000 feet occurs because the ambient temperature becomes constant at about this altitude. The figure indicates that at altitudes above 53 000 feet a new stainless-steel aircraft ( $\epsilon = 0.1$ ) flying at Mach 6 would have a higher wall temperature than an older stainless-steel aircraft ( $\epsilon = 0.9$ ) flying at Mach 9.

The skin-friction ratios, corresponding to the wall temperatures of figure 7, are presented in figure 8. Again, the ratio  $C_F/C_{F,aw}$  indicates the amount of deviation from the adiabatic-wall conditions.

This figure indicates that a supersonic-transport-type aircraft, with stainless-steel skin and a cruise Mach number of 3, would have about 3.6 percent higher skin-friction drag after several flights ( $\epsilon = 0.9$ ) than when it was new and unoxidized ( $\epsilon = 0.1$ ). This percentage increases rapidly with Mach number such that the difference is about 16 percent at Mach 9. Between the oxidized stainless steel ( $\epsilon = 0.9$ ) and the oxidized titanium ( $\epsilon = 0.5$ ) the skin-friction difference increases from about 2.4 percent at Mach 3 to about 3.7 percent at Mach 9.

The preceding discussion indicates that an increase in wall temperature leads to a decrease in skin friction. However, the structural advantages of low skin temperature are essential and heavily outweigh the disadvantage of the increased skin friction associated with the low wall temperature. The object of this report is to point out that these skin-friction increments are present and should be accounted for when drag estimates are made.

The last part of this study concerns the altitude effect on wall temperature and skin friction for several values of emittance. Figure 7 shows the average wall temperature as a function of altitude for several Mach numbers and values of emittance. The curve for  $M = 0$  simply represents the ambient temperature at the specified altitude.

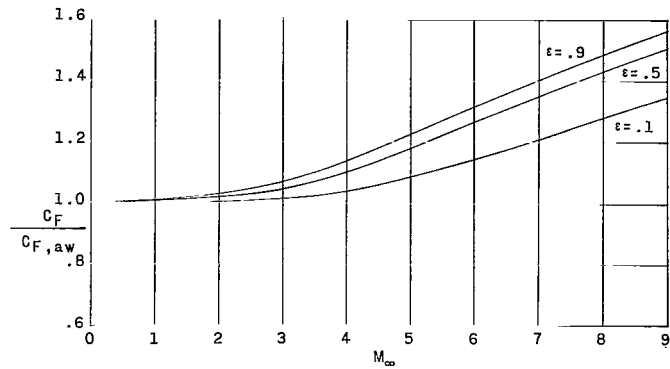


Figure 6. - Effect of emittance and Mach number on average skin-friction ratio.  $H = 75\,000$  feet;  $L = 200$  feet.

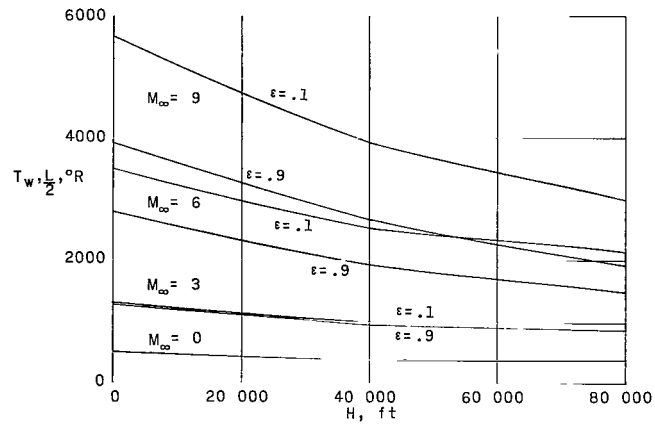


Figure 7. - Variation of average wall temperature with altitude, Mach number, and emittance.  $L = 200$  feet.

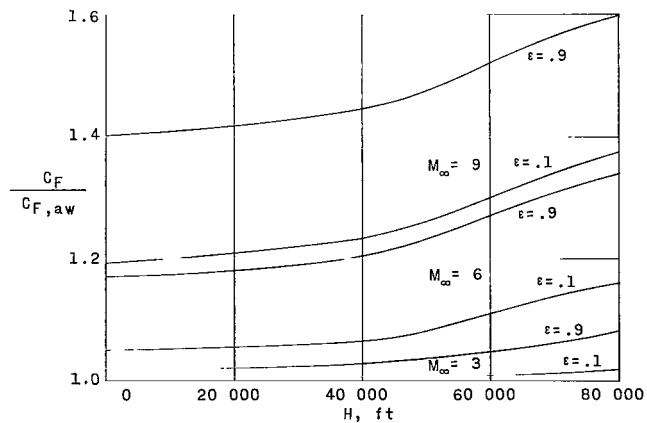


Figure 8. - Variation of average skin-friction ratio with altitude, Mach number, and emittance.  $L = 200$  feet.

## CONCLUDING REMARKS

A search of available literature indicates that the radiative properties of supersonic aircraft materials depend heavily upon the metal chosen for the aircraft skin and the degree of oxidation of the surface. A calculative study has been made to determine the effect of emittance upon wall temperature and skin friction over a range of supersonic and low hypersonic flight conditions. Calculations were made for Mach numbers up to 9, altitudes up to 80 000 feet, and vehicle lengths up to 200 feet.

The results indicate that the skin-friction drag of a supersonic aircraft increases with increased surface emittance. Emittance increases with surface oxidation. Thus, for a new supersonic aircraft with skin made of a metal with low radiative properties in the polished, unoxidized state, the skin-friction drag will increase with time until the surface becomes stably oxidized. This effect of emittance on skin friction increases with Mach number and becomes substantial above Mach numbers of about 2.5. Hence, for specified flight conditions, the level of skin-friction drag at which the vehicle operates depends upon the metal used for the skin of the aircraft and the degree of oxidation of the metal.

Langley Research Center,  
National Aeronautics and Space Administration,  
Langley Station, Hampton, Va., November 25, 1964.

## REFERENCES

1. Truitt, Robert Wesley: Fundamentals of Aerodynamic Heating. The Ronald Press Co., c.1960.
2. Sommer, Simon C.; and Short, Barbara J.: Free-Flight Measurements of Turbulent-Boundary-Layer Skin Friction in the Presence of Severe Aerodynamic Heating at Mach Numbers From 2.8 to 7.0. NACA TN 3391, 1955.
3. Dobbins, John P.: Emittances of Titanium, Aluminum, and Stainless Steel. Rept. No. NA-49-238, North Am. Aviation, Inc., Mar. 25, 1949.
4. Wood, W. D.; Deem, H. W.; and Lucks, C. F.: The Emittance of Stainless Steels. DMIC Mem. 111 (OTS PB 171630), Battelle Mem. Inst., June 12, 1961.
5. Slemp, Wayne S.: Effects of Preoxidation Treatments on Spectral Normal and Total Normal Emittance of Inconel, Inconel-X, and Type 347 Stainless Steel. NASA TN D-2300, 1964.
6. Hodgman, Charles D.; Weast, Robert C.; and Selby, Samuel M., eds.: Handbook of Chemistry and Physics. Forty-first ed., Chemical Rubber Pub. Co., 1959-1960.
7. Bryant, J. M.; Roach, R. E.; and Donaldson, J. E.: Physical Properties of Aircraft Structural Materials at Elevated Temperatures. Rept. No. 9112, Vol. I, Chance Vought Aircraft, Inc., June 1, 1955.
8. Singham, J. R.: Tables of Emissivity of Surfaces. Intern. J. Heat Mass Transfer, vol. 5, Jan.-Feb. 1962, pp. 67-76.
9. Gelinas, R. W.: An Estimate of the Infrared Radiation From a Supersonic Bomber. U.S. Air Force Proj. RAND Paper S-75 (ASTIA Doc. No. AD 150671), The RAND Corp., Mar. 5, 1958.

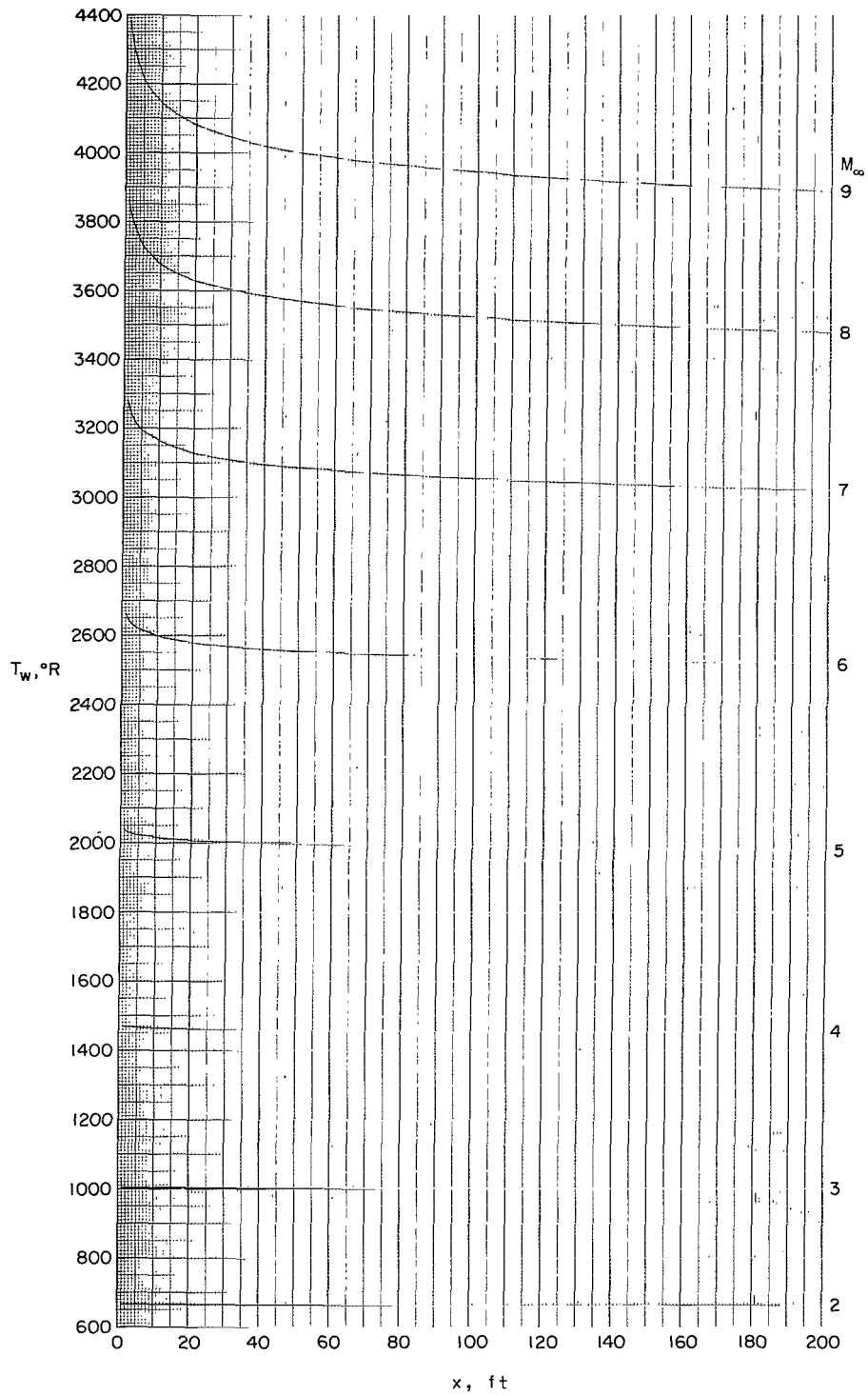


# APPENDIX

This appendix is presented as an aid to the aircraft designer in calculating equilibrium wall temperature and, hence, skin friction. The computations were made in the same manner described previously in the section "Method of Calculation." Calculations of the distribution of equilibrium wall temperatures for vehicle lengths up to 200 feet were made for Mach numbers from 2 to 9, emittances from 0.1 to 0.9, and altitudes from 40 000 to 120 000 feet. The local wall equilibrium temperature  $T_w$  is plotted in figures A-1 to A-5 as a function of surface distance  $x$  and Mach number  $M_\infty$ . The altitudes and ratios  $\frac{R/ft}{M_\infty}$  corresponding to the various figures are indicated in the following table:

Figure	H, ft	$\frac{R/ft}{M_\infty}$
A-1 . . . . .	40 000	$1.925 \times 10^6$
A-2 . . . . .	60 000	$7.393 \times 10^5$
A-3 . . . . .	80 000	$2.789 \times 10^5$
A-4 . . . . .	80 000	$1.070 \times 10^5$
A-5 . . . . .	120 000	$4.076 \times 10^4$

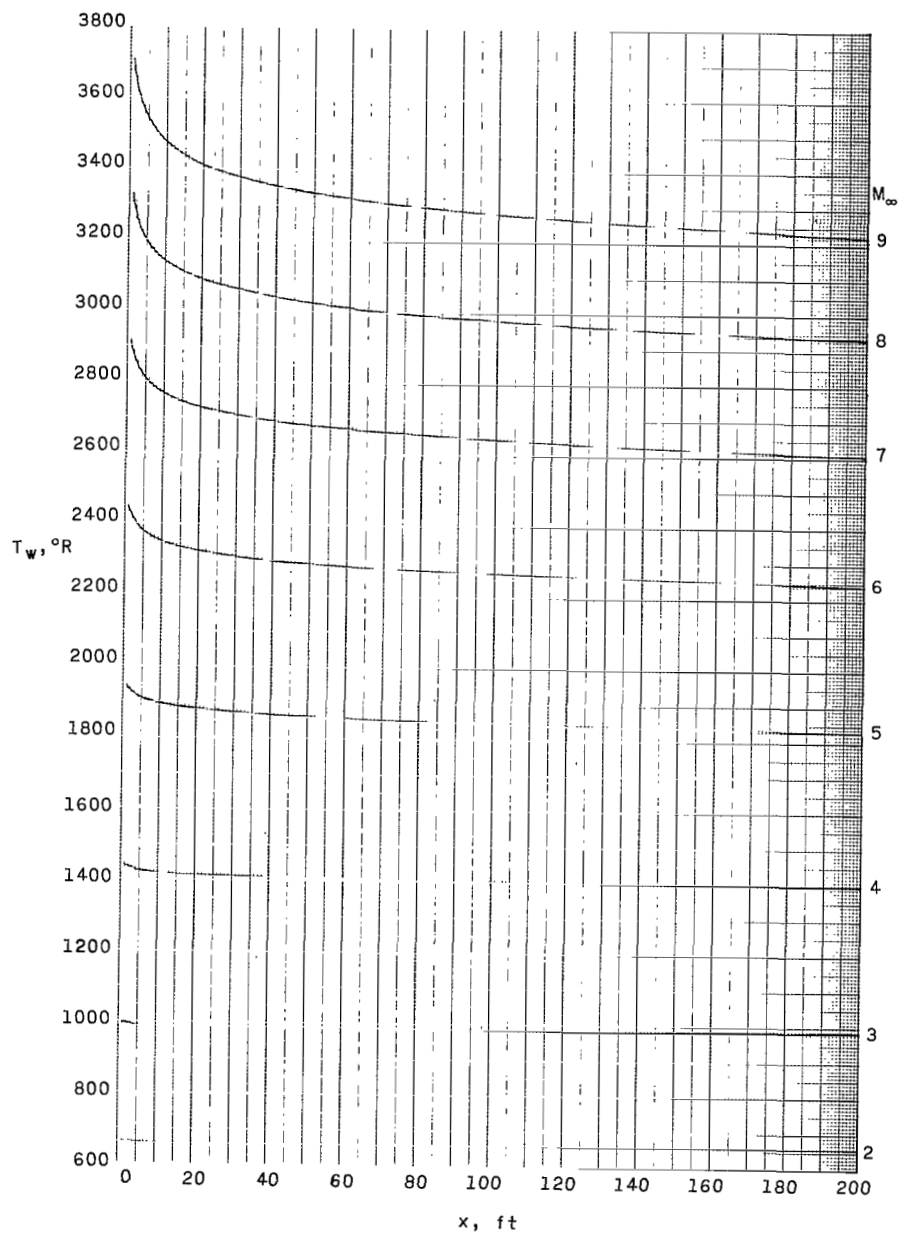
# APPENDIX



(a)  $\varepsilon = 0.1$ .

Figure A-1.- Variation of equilibrium local wall temperature with surface distance.  $H = 40\,000$  feet;  $\frac{R/ft}{M_\infty} = 1.925 \times 10^6$ .

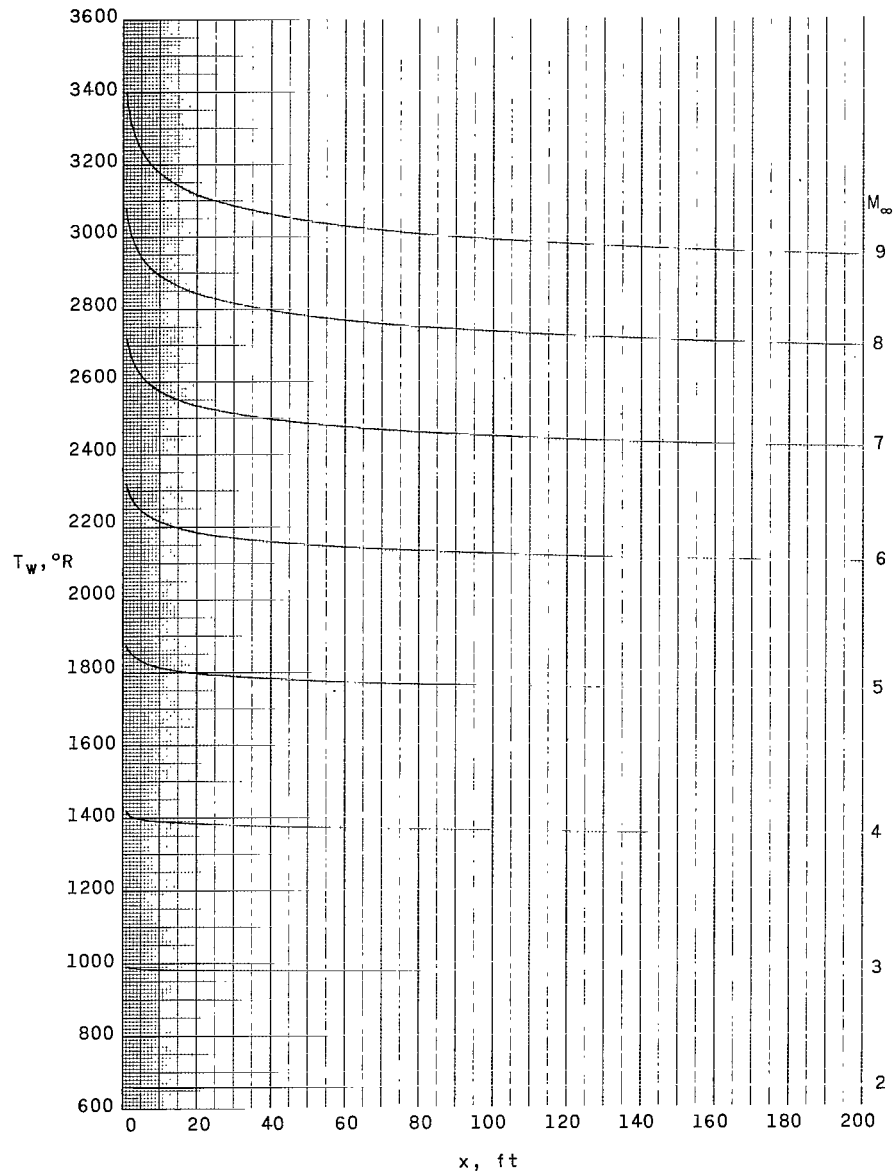
# APPENDIX



(b)  $\varepsilon = 0.3$ .

Figure A-1.- Continued.

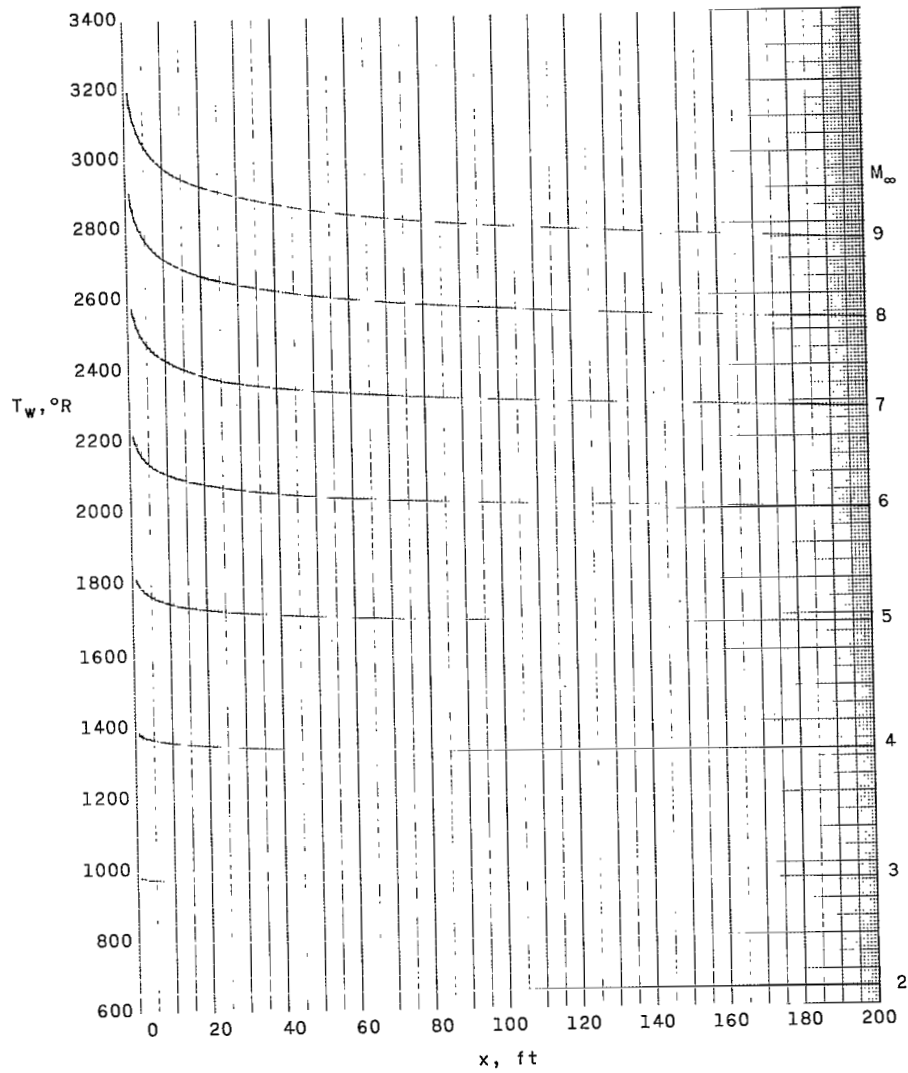
# APPENDIX



(c)  $\varepsilon = 0.5$ .

Figure A-1.- Continued.

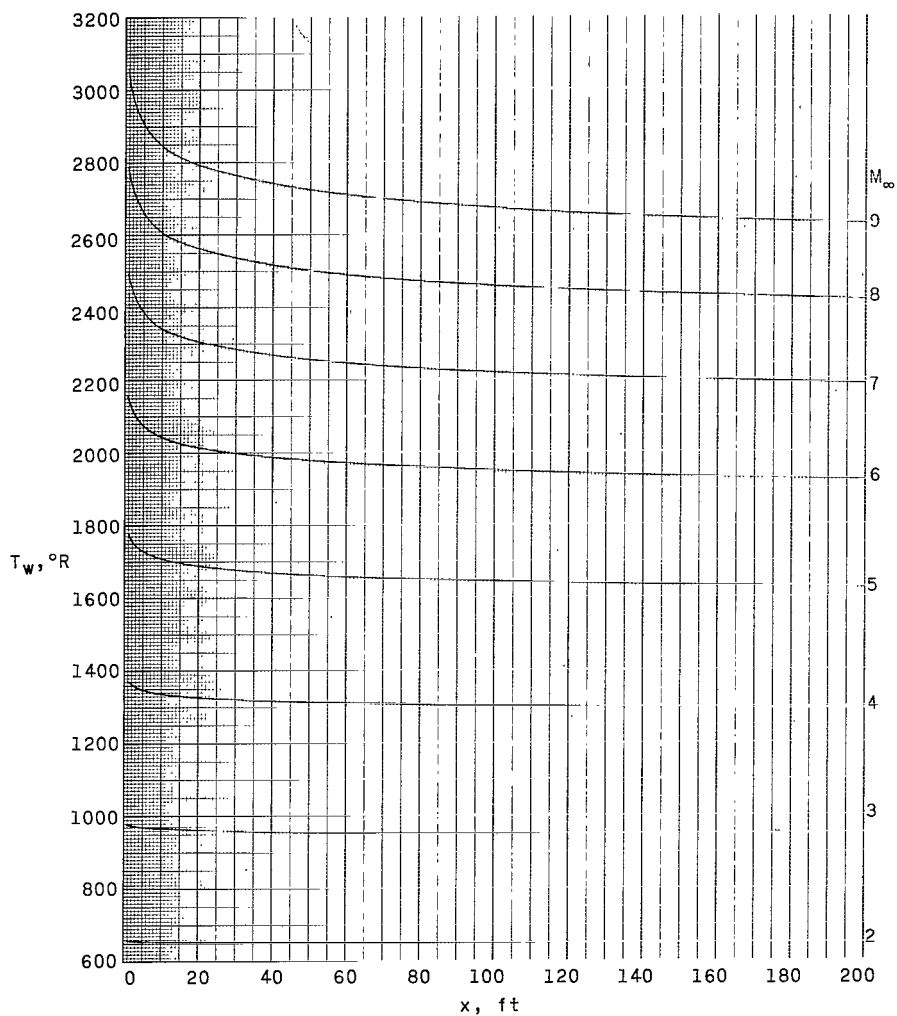
# APPENDIX



(d)  $\epsilon = 0.7$ .

Figure A-1.- Continued.

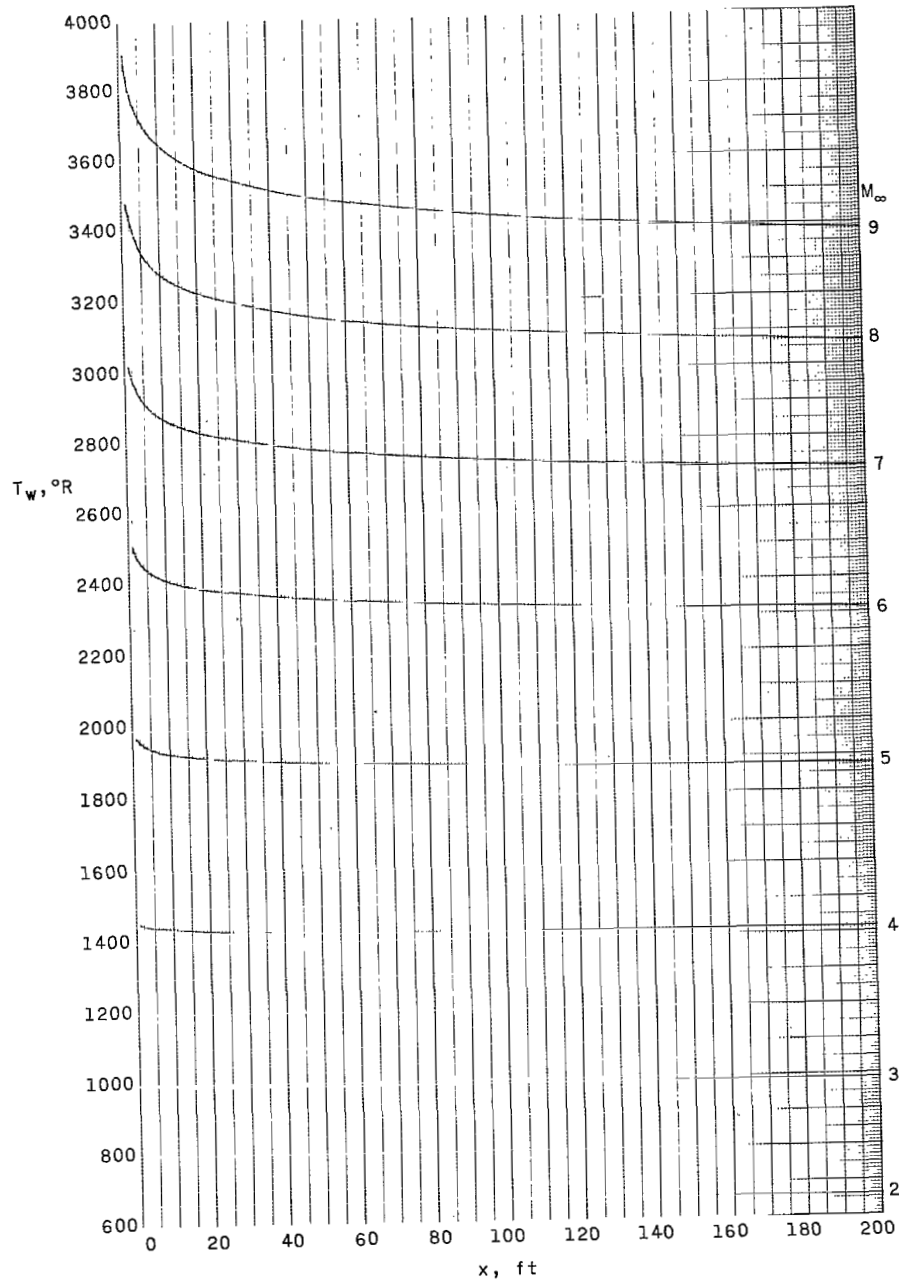
# APPENDIX



(e)  $\epsilon = 0.9$ .

Figure A-1.- Concluded.

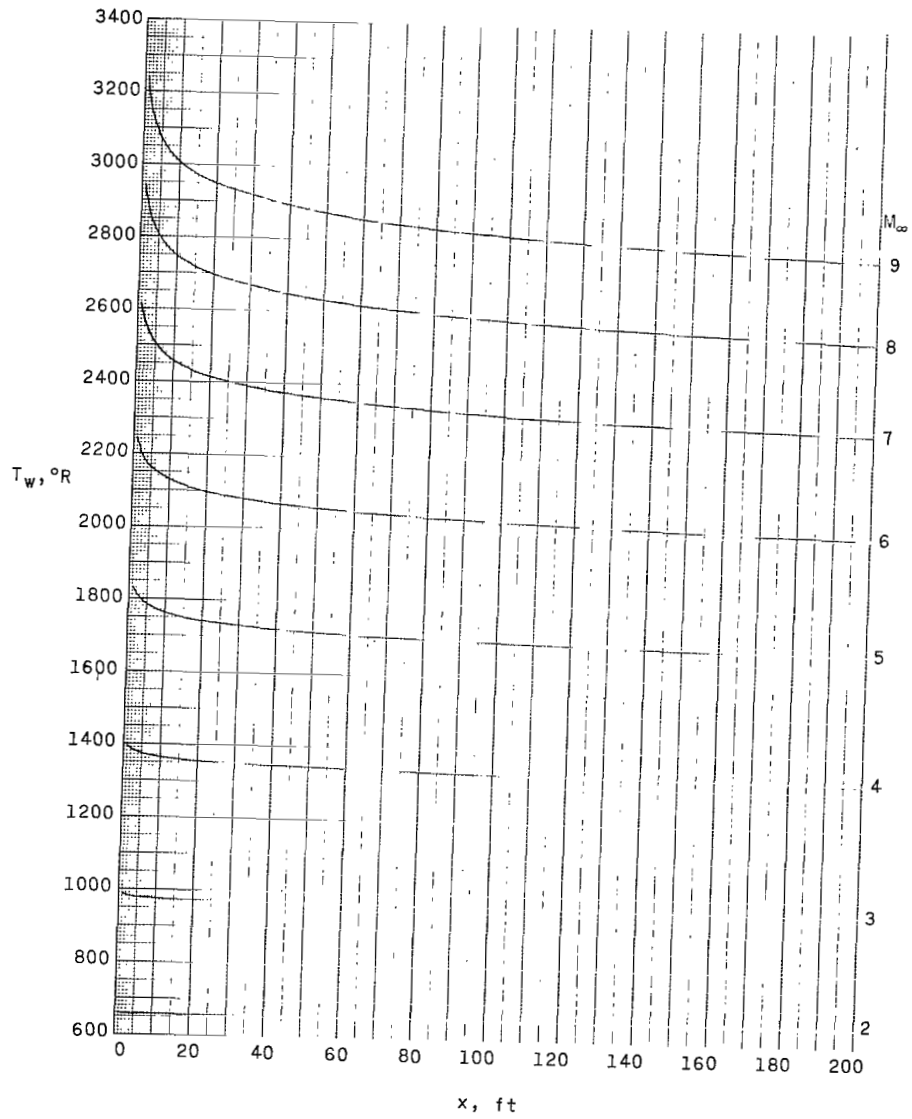
# APPENDIX



(a)  $\epsilon = 0.1$ .

Figure A-2.- Variation of equilibrium local wall temperature with surface distance.  $H = 60\,000$  feet;  $\frac{R/ft}{M_\infty} = 7.393 \times 10^5$ .

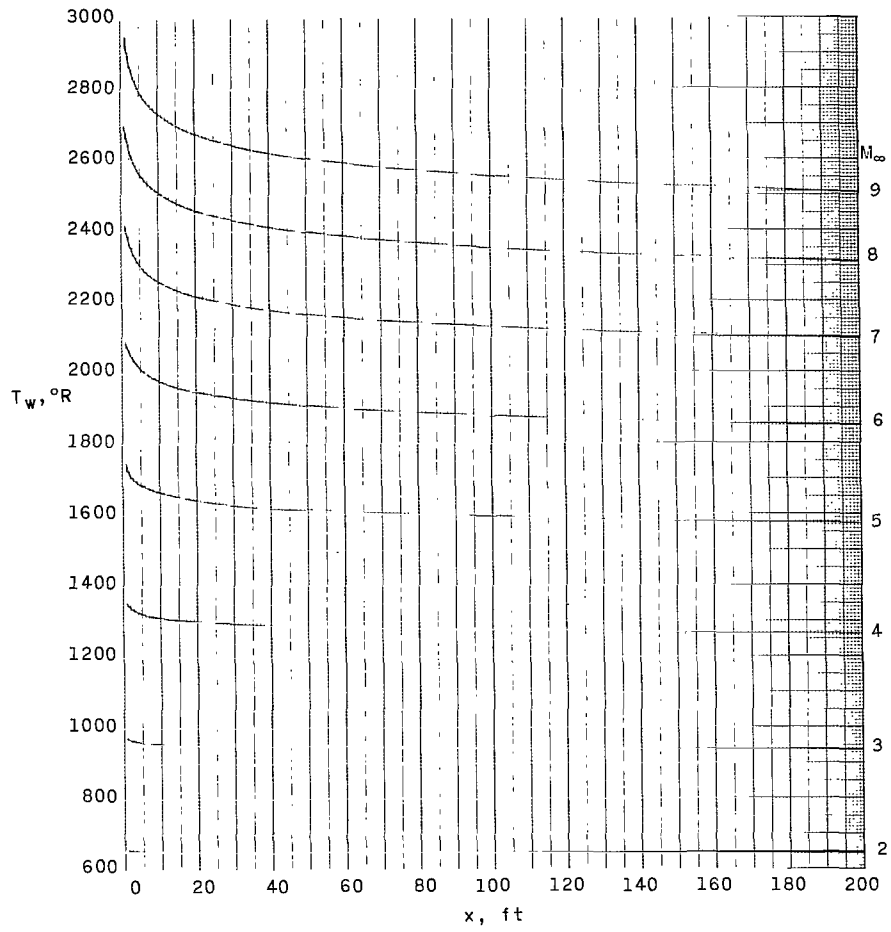
# APPENDIX



(b)  $\epsilon = 0.3$ .

Figure A-2.- Continued.

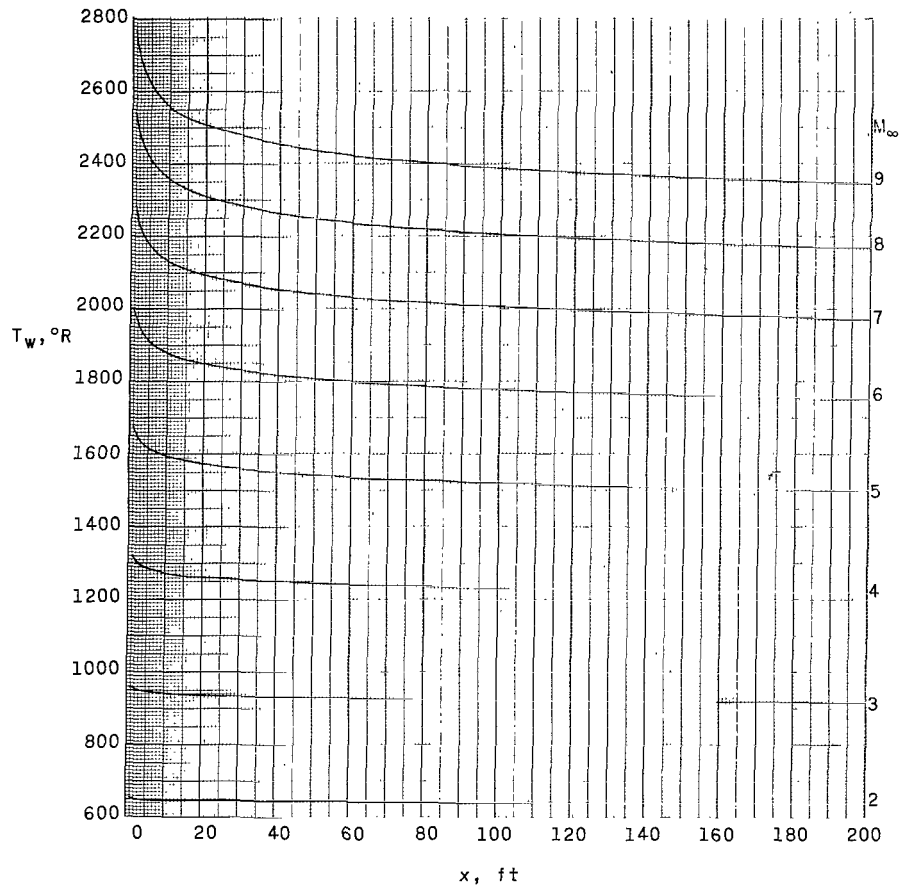
# APPENDIX



(c)  $\epsilon = 0.5$ .

Figure A-2.- Continued.

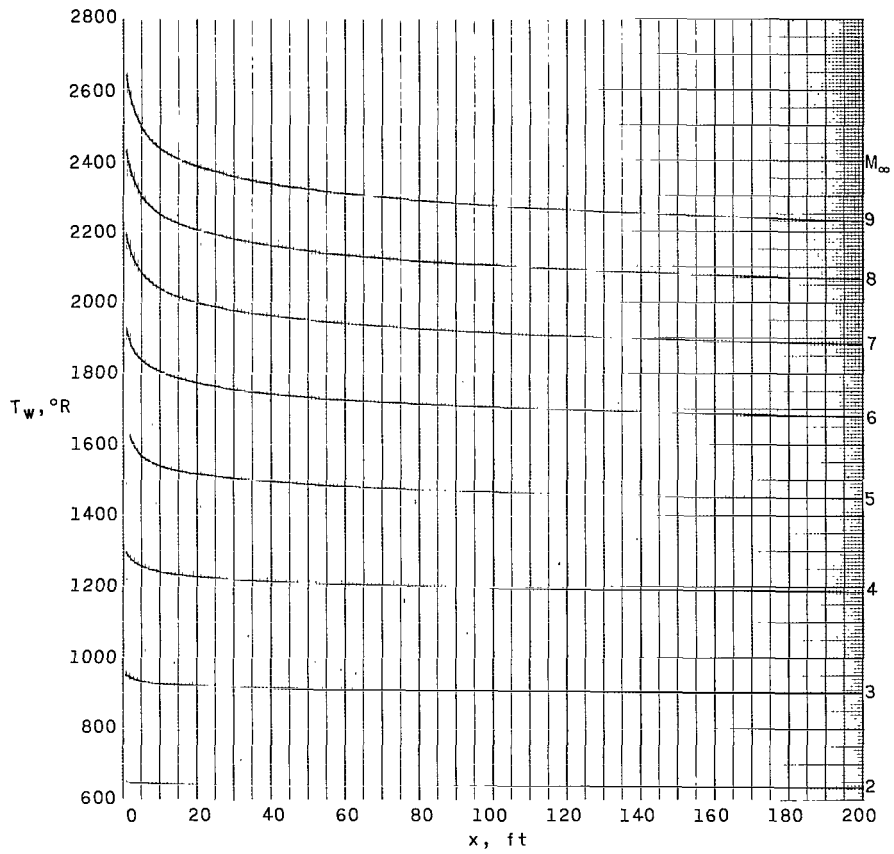
# APPENDIX



(d)  $\epsilon = 0.7$ .

Figure A-2.- Continued.

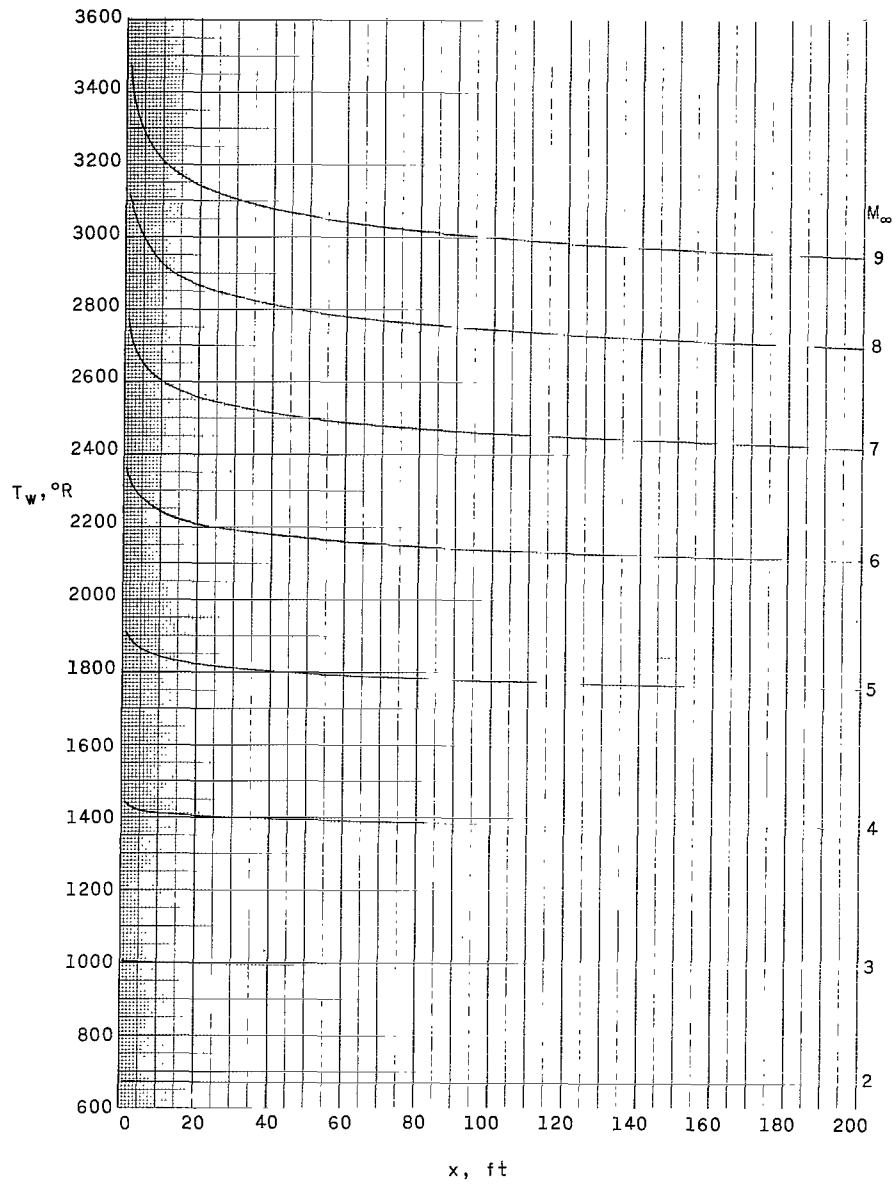
# APPENDIX



(e)  $\varepsilon = 0.9$ .

Figure A-2.- Concluded.

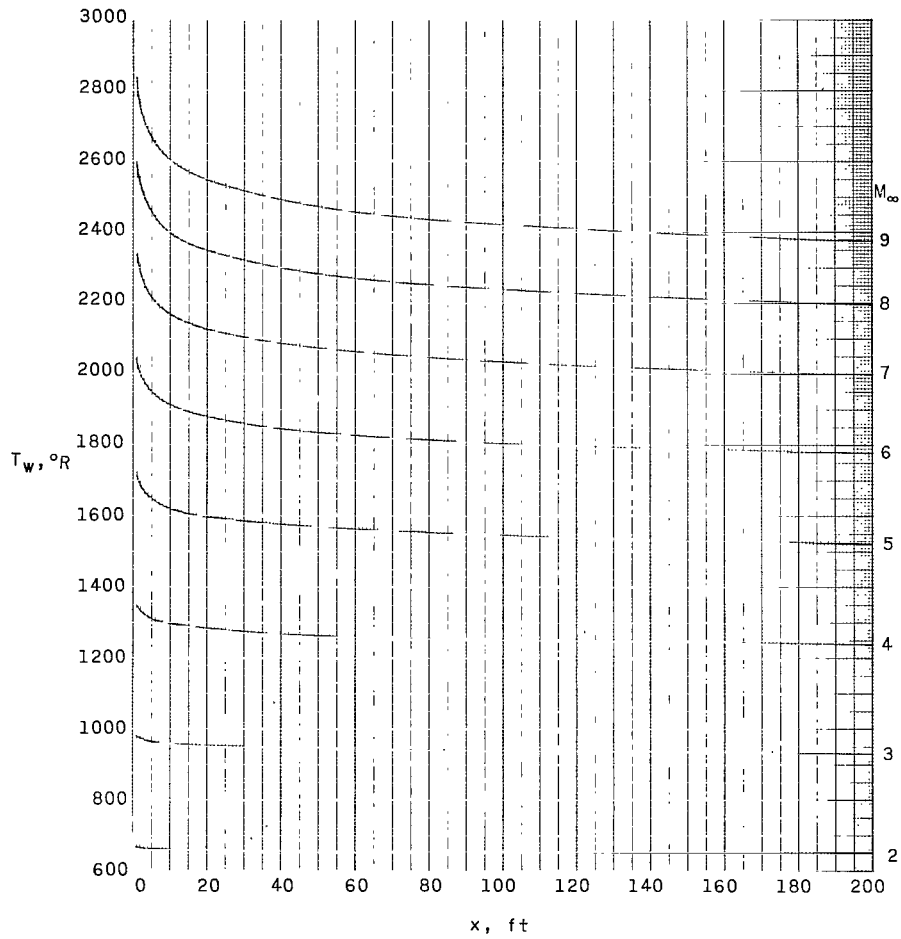
# APPENDIX



(a)  $\varepsilon = 0.1$ .

Figure A-3.- Variation of equilibrium local wall temperature with surface distance.  $H = 80\,000$  feet;  $\frac{R/ft}{M_\infty} = 2.789 \times 10^5$ .

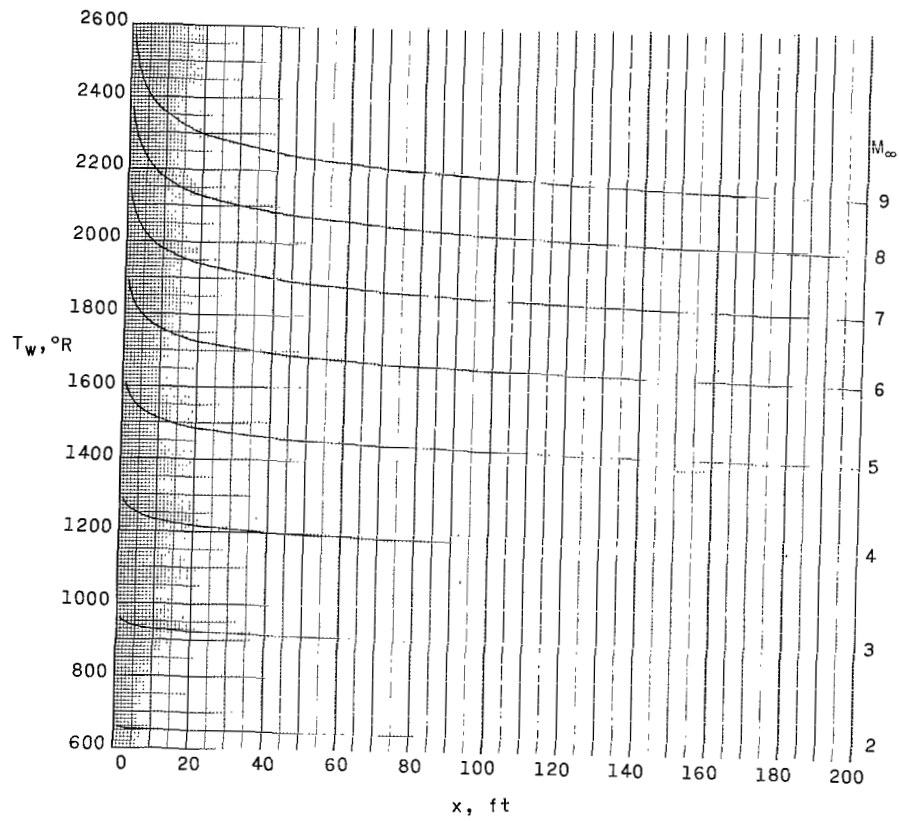
# APPENDIX



(b)  $\epsilon = 0.3$ .

Figure A-3.- Continued.

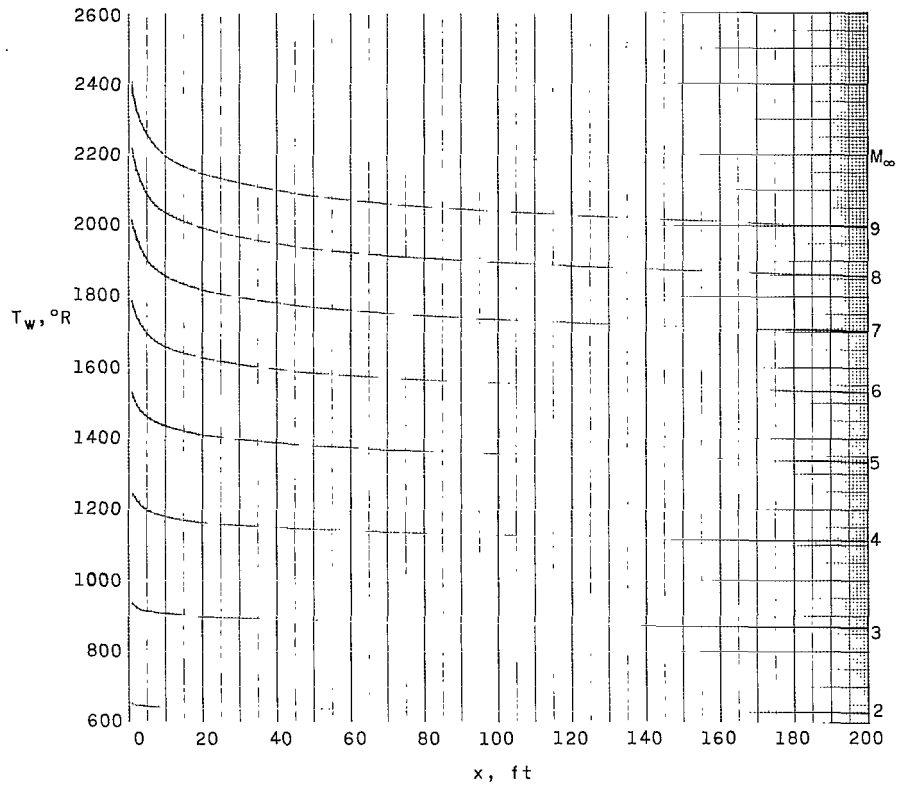
# APPENDIX



(c)  $\epsilon = 0.5$ .

Figure A-3.- Continued.

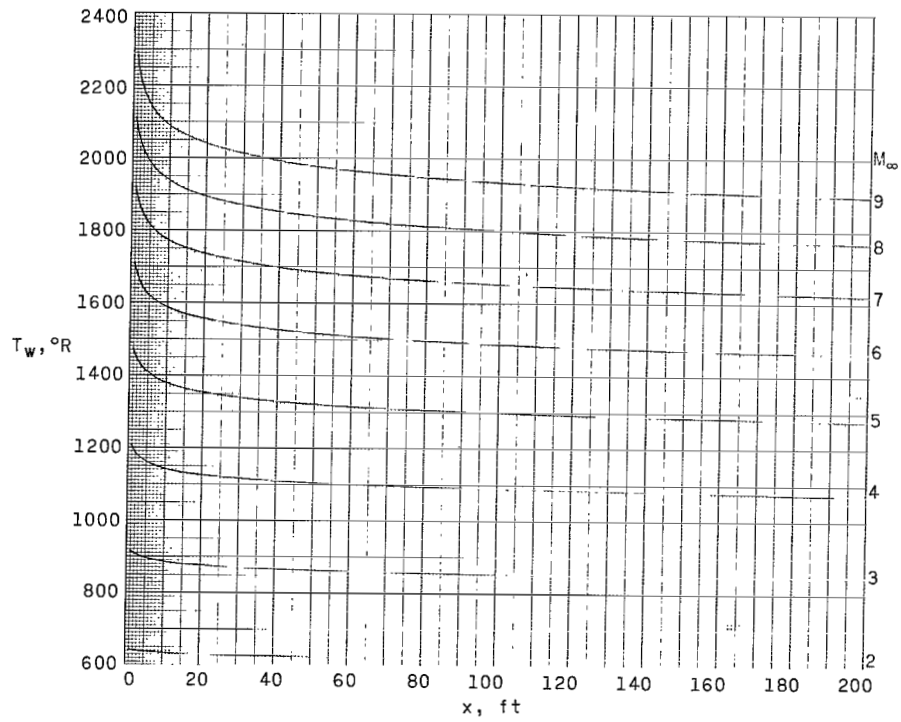
# APPENDIX



(d)  $\epsilon = 0.7$ .

Figure A-3.- Continued.

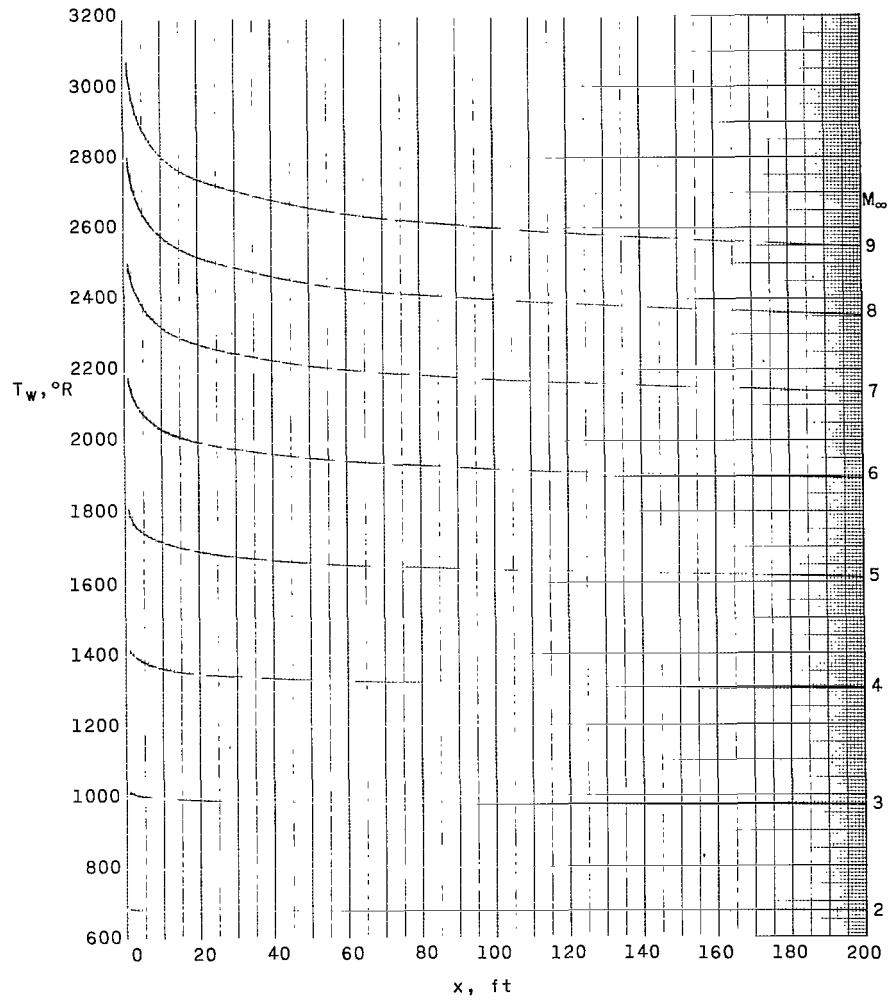
# APPENDIX



(e)  $\varepsilon = 0.9$ .

Figure A-3.- Concluded.

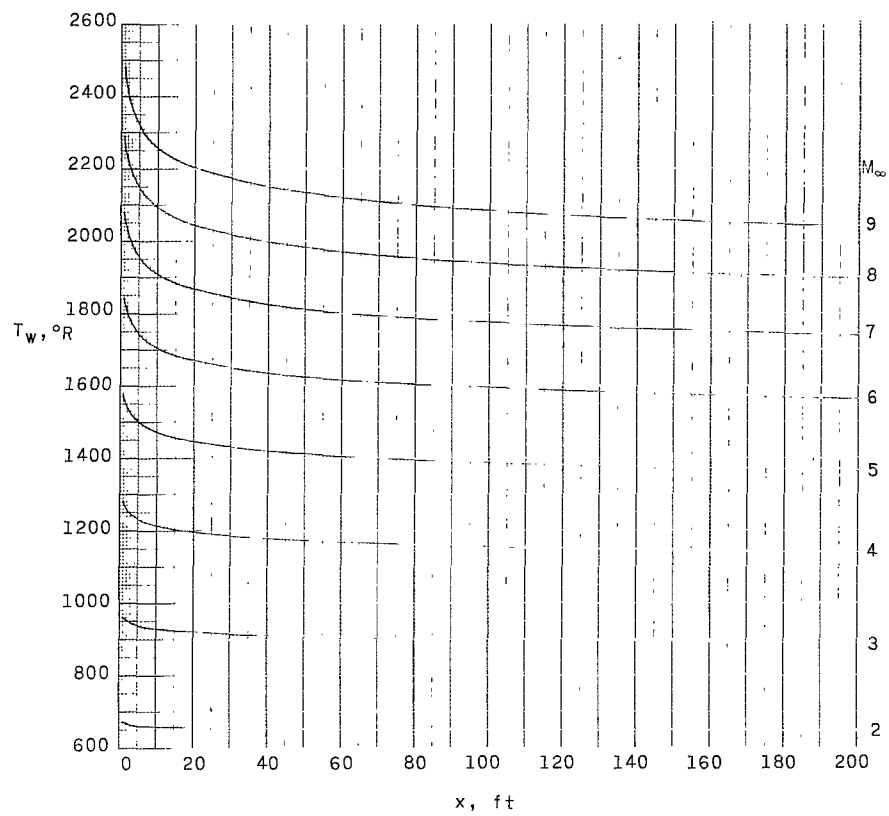
# APPENDIX



(a)  $\epsilon = 0.1$ .

Figure A-4.- Variation of equilibrium local wall temperature with surface distance.  $H = 80\,000$  feet;  $\frac{R}{ft} = 1.070 \times 10^5$ .

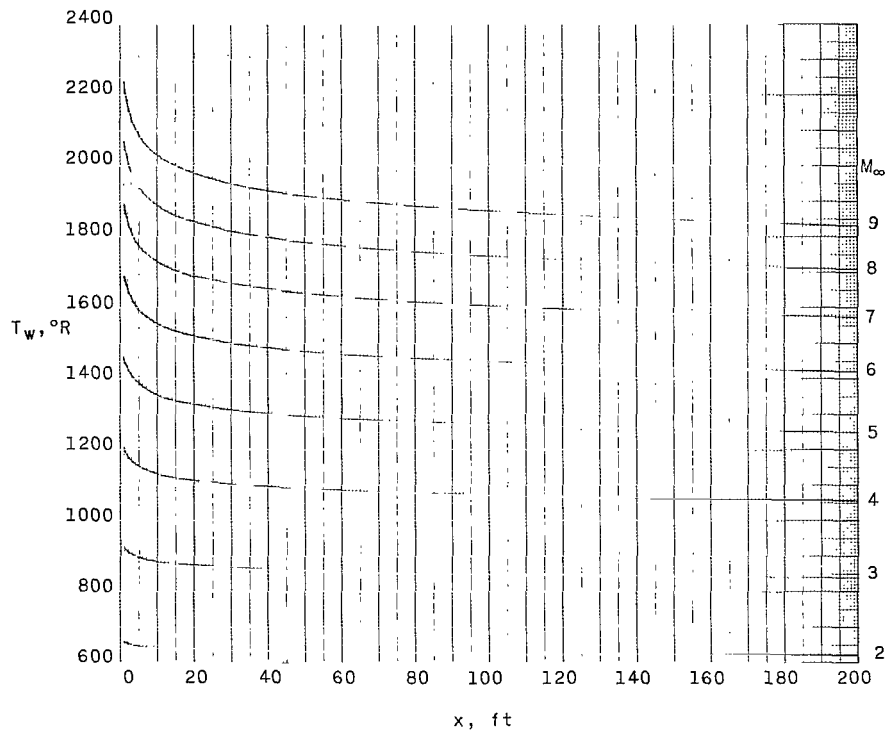
# APPENDIX



(b)  $\epsilon = 0.3$ .

Figure A-4.- Continued.

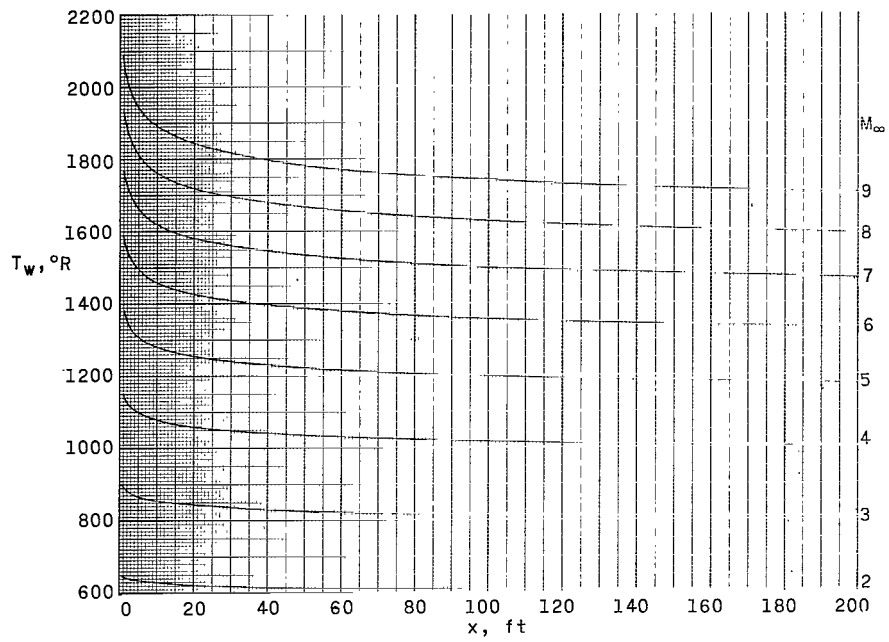
# APPENDIX



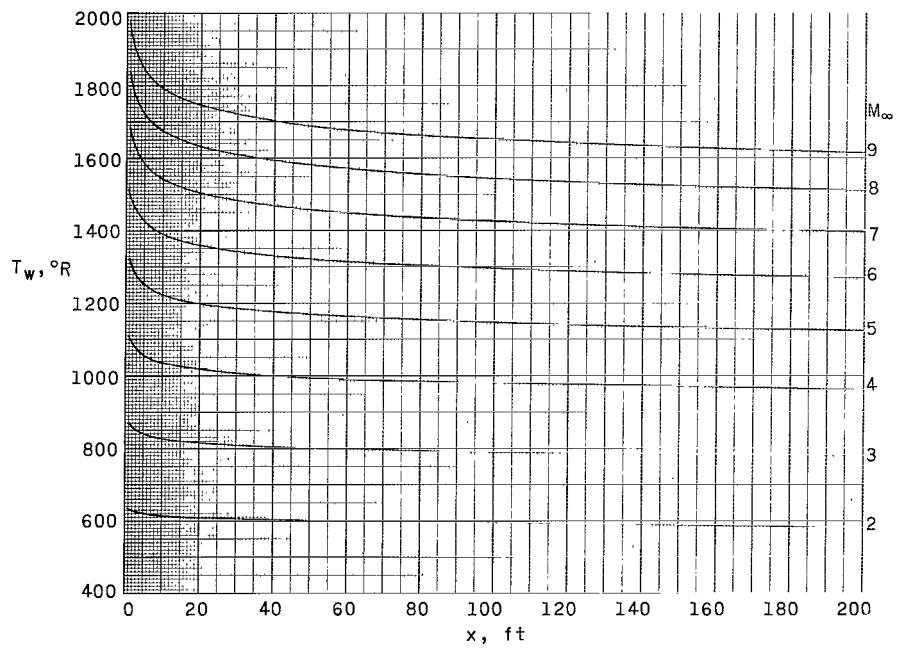
(c)  $\varepsilon = 0.5$ .

Figure A-4.- Continued.

# APPENDIX



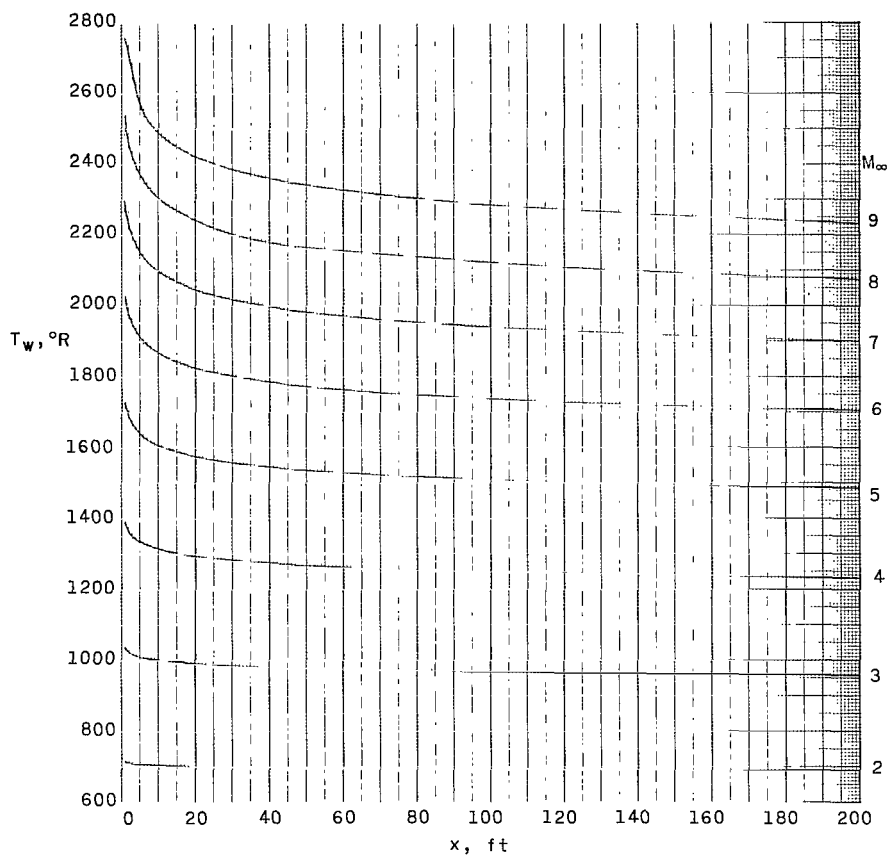
(d)  $\varepsilon = 0.7$ .



(e)  $\varepsilon = 0.9$ .

Figure A-4.- Concluded.

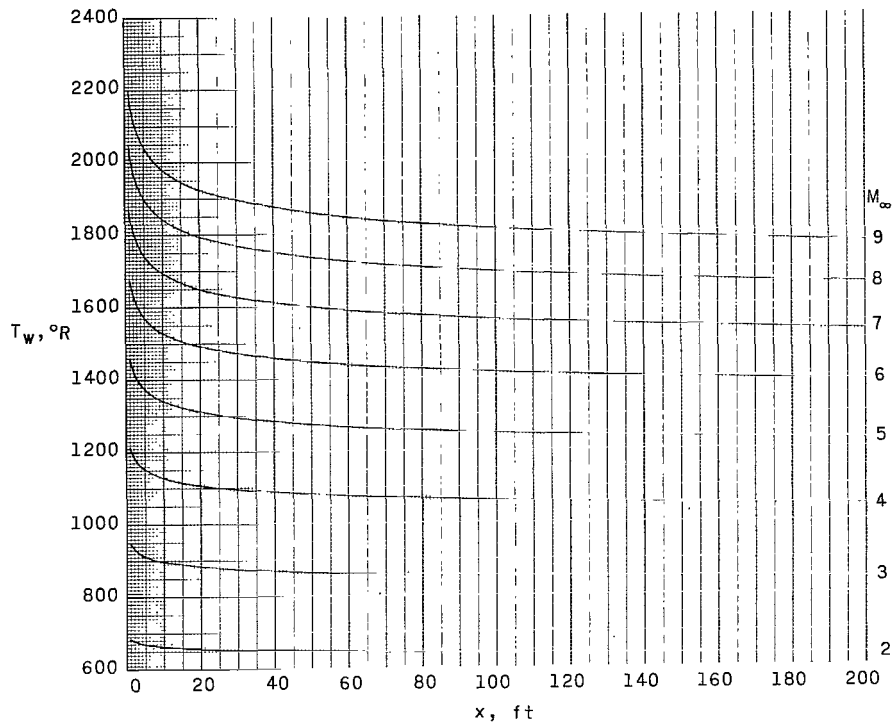
# APPENDIX



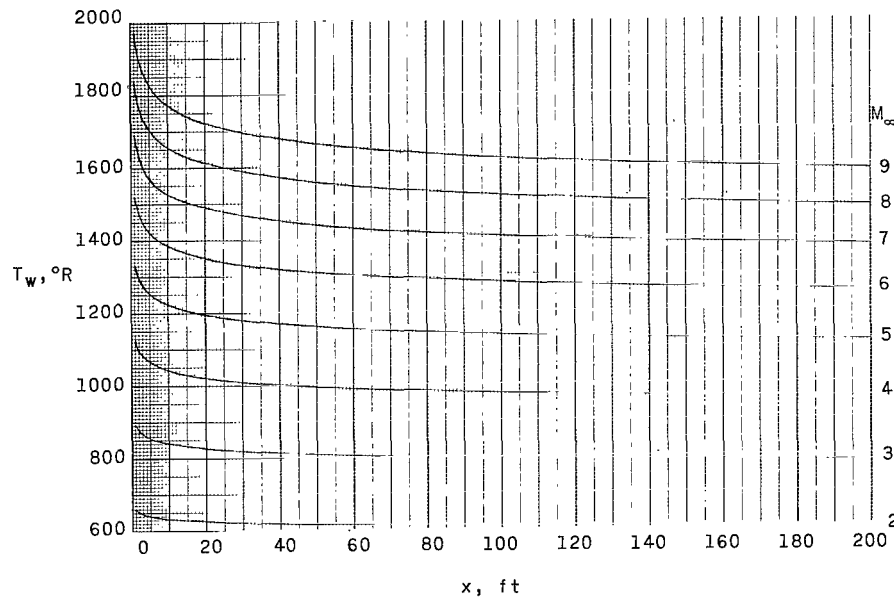
(a)  $\varepsilon = 0.1$ .

Figure A-5.- Variation of equilibrium local wall temperature with surface distance.  $H = 120\,000$  feet;  $\frac{R/ft}{M_\infty} = 4.076 \times 10^4$ .

# APPENDIX



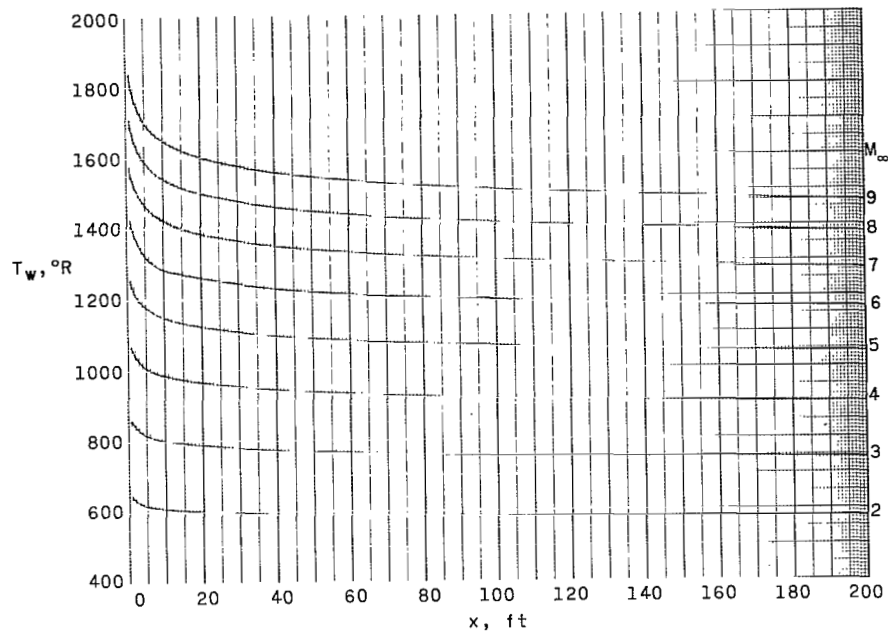
(b)  $\varepsilon = 0.3$ .



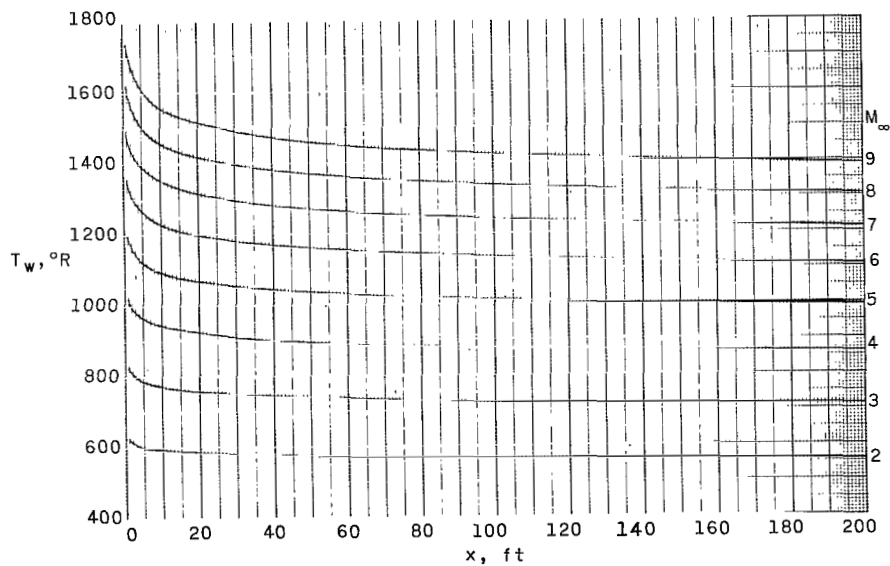
(c)  $\varepsilon = 0.5$ .

Figure A-5.- Continued.

# APPENDIX



(d)  $\epsilon = 0.7$ .



(e)  $\epsilon = 0.9$ .

Figure A-5.- Concluded.

2/22/85  
[Signature]

*"The aeronautical and space activities of the United States shall be conducted so as to contribute . . . to the expansion of human knowledge of phenomena in the atmosphere and space. The Administration shall provide for the widest practicable and appropriate dissemination of information concerning its activities and the results thereof."*

—NATIONAL AERONAUTICS AND SPACE ACT OF 1958

## NASA SCIENTIFIC AND TECHNICAL PUBLICATIONS

**TECHNICAL REPORTS:** Scientific and technical information considered important, complete, and a lasting contribution to existing knowledge.

**TECHNICAL NOTES:** Information less broad in scope but nevertheless of importance as a contribution to existing knowledge.

**TECHNICAL MEMORANDUMS:** Information receiving limited distribution because of preliminary data, security classification, or other reasons.

**CONTRACTOR REPORTS:** Technical information generated in connection with a NASA contract or grant and released under NASA auspices.

**TECHNICAL TRANSLATIONS:** Information published in a foreign language considered to merit NASA distribution in English.

**TECHNICAL REPRINTS:** Information derived from NASA activities and initially published in the form of journal articles.

**SPECIAL PUBLICATIONS:** Information derived from or of value to NASA activities but not necessarily reporting the results of individual NASA-programmed scientific efforts. Publications include conference proceedings, monographs, data compilations, handbooks, sourcebooks, and special bibliographies.

*Details on the availability of these publications may be obtained from:*

SCIENTIFIC AND TECHNICAL INFORMATION DIVISION  
NATIONAL AERONAUTICS AND SPACE ADMINISTRATION  
Washington, D.C. 20546